Measurements to Estimate the Downward Heat Flux from a Burning Oil Pool

Chris Petrich[1], Megan O'Sadnick[1], Nga P. Dang[1],
Linda Marie Stakkeland[2], Steffen Kristiansen[2]
(1) Northern Research Institute (Norut) Narvik, Narvik, Norway
(2) Norwegian Fire Academy, Fjelldal, Norway
christian.petrich@norut.no

Abstract

Oil spills in ice-covered waters pose unique challenges to remediation activities. In-situ burning is a potential remediation technique that has shown promising efficiency in earlier trials. An element of in-situ burning is the feedback between the flame of a burn on ice and the melting, oil-infiltrated ice beneath. To measure the vertical downward heat flux, a series of burns were performed on a concrete platform instrumented with temperature sensors. The oil pool had a diameter of 200 mm and burn times were between 5 and 15 minutes. The heat flux was determined beneath the pool at the center of the platform. The heat flux into the platform increased with time, reaching 10 to 15 kW/m^2 beneath the flame during burns of crude oil, Diesel, and intermediate fuel oil (IFO 60). The heat flux from crude oil burning on a pool of water was up to 1 kW/m^2 prior to the vigorous burn phase (boil-over), and 5 kW/m^2 during that phase. The measurements provide a constraint for experiment design and modeling of in-situ burning of oil on ice.

1 Introduction

In-situ burning of oil on ice is a potential remediation technique (Buist et al., 2013). Investigation have been performed of feedbacks from a flame on vertical ice walls, for example in ice cavities and at the edge of leads (e.g., Bellino et al., 2013; Farahani et al., 2017; Shi et al., 2017). However, there seems to be only one estimate of the downward heat flux through an oil slick into underlying water, finding 2.5 kW/m^2 (Evans et al., 1988). Sea ice has been found to contain up to 5% oil in its pore structure (cf. NORCOR, 1975), so the downward heat flux from the flame may be a driver for supplemental oil release during in-situ burning on oil-infested sea ice. The energy balance of a burn is comprised of evaporation and combustion linked by radiative and conductive heat transfer (Buist et al., 2013). Many burn parameters depend somewhat on the size of the burn (Garo et al., 1999; Buist et al., 2013). The goal of this work was to infer the conductive heat flux into the ground beneath a small oil pool fire. While the ultimate application is to fires on ice, the present measurements were performed on mortar.

2 Methods

Four burns were conducted in sequence in a burn pan. The burn pan was embedded in a block made from refractory mortar with 23 % m/m water content in the original mixture. The block dimensions were 300 x 300 x 75 mm^3, surrounded by 50 mm Styrofoam insulation (Figure 1). The block was constructed seven days before the burns. The burn pan had a diameter of 200 mm and was 20 mm deep. K-type thermocouples were embedded at the center of the block, at 0, 5, 10, 15, 20, and 25 mm from the bottom of the pan, respectively. Temperatures were logged every 10 seconds with a Campbell Scientific CR1000 data logger. During the last two burns, an additional thermocouple had been placed in the lower part of the flame. No readings were obtained from the temperature sensor at 25 mm.

To calculate the next downward heat flux into the block, the temperature in the lower part of the block was estimated with the help of a one-dimensional heat conduction model. The model was driven by the temperatures recorded at the 5-mm position (the sensor at the 0 mm position was not used due to surface damage inflicted during the second burn) with adiabatic bottom boundary, and using a thermal diffusivity of κ=6.4 × 10^{-7} m^2/s. The following equation was solved implicitly

$$\frac{dT}{dt} = \kappa \frac{d^2T}{dz^2} \quad [1]$$

The thermal diffusivity was tuned manually to optimize agreement between model and data.

The heat flux into the block, *F*, was calculated as the time derivate of the enthalpy of the block, i.e.,

$$F = \frac{dH}{dt} = \frac{d}{dt} \rho c \int T(z) dz \quad [2]$$

where $T(z)$ is the temperature at position z, H is the enthalpy, and ρc =1.8 MJ m^{-3} K^{-1} is the volumetric heat capacity of the mortar. The integral was solved in two different ways due to uncertain reliability of the surface measurement (T_0) since burn 2 (see Results),

$$\int T(z) dz = 0.02 \text{ m } \frac{0.5\, T_0 + T_5 + T_{10} + T_{15} + 0.5\, T_{20}}{4} + \sum_{20 \text{ mm}}^{55 \text{ mm}} T\, \Delta z \quad [3]$$

where the temperatures in the sum on the right hand were modeled and the subscripted temperatures are measured at the respective depth, or, excluding the temperature reading at the surface (T_0),

$$\int T(z) dz = 0.02 \text{ m } \frac{T_5 + T_{10} + T_{15} + 0.5\, T_{20}}{3.5} + \sum_{20}^{55} T\, \Delta z \quad [4]$$

A sequence of four burns had been performed at the premises of the Norwegian Fire Academy, using (1) crude oil, (2) Diesel, (3) intermediate fuel oil IFO-60, and (4) crude oil on water (Table 1) on 31 May 2017. Ignition was performed with a blow torch. The ambient air temperature was 10 °C and winds were gusting up to 2 m/s.

3 Results

Experiments were performed on an overcast day with intermittent slight drizzle and ambient temperatures around 6 °C (Figure 2). The temperature of the base was 5.5 °C before the first burn, and 80 °C after the last burn (Figure 3).

3.1 Burn 1

500 mL of crude oil (approx. 435 g) were added to the pan. Oil and base temperature were approximately 6 °C, and the oil was ignited within 5 seconds. Gusts during the first burn set the lateral insulation on fire 1 minute after ignition. The smoldering insulation was extinguished 3.5 minutes after ignition. Bubbles started to penetrate the oil 7.5 minutes after ignition, more

than doubling the oil volume for about 20 seconds. Bubbles presumably originated from water vapor released from the freshly cured cement block. The burn terminated 9:20 minutes after ignition. The highest temperature measured in the base was 140 °C. No re-ignition was attempted. The oil residue was removed with absorbent paper, extracted with heptane, and left to evaporate for 1 month at room temperature. At that point the residue mass was 74 g with a density of 920 kg/m^3.

3.2 Burn 2

450 mL Diesel were burned in the pan. The base temperature was 30 °C prior to addition of the Diesel sample. The burn lasted for 12 minutes. 11 minutes into the burn, two small bits of mortar were ejected from the bottom of the pan (total 24 g). One bit originated close to the temperature probe (sensor T_0). The Diesel sample burned or evaporated completely and left no residue. The highest temperature recorded in the base was 300 °C. The source of the explosion was probably an increase in pore vapor pressure in response to the high temperature of the mortar. Specifically, the water vapor pressure at 300 °C is 8.5 MPa, i.e. 85 times atmospheric pressure.

3.3 Burn 3

Starting with a base at 50 °C, 500 mL IFO-60 fuel oil were ignited without problem. 12:50 minutes after ignition, bubbles penetrated the oil, oil started to ooze out of the pan and the flame was blown out. Temperatures in the pan reached 230 °C. Reignition was attempted 4 minutes later. A self-sustained flame was obtained that burned for 1 minute until bubbles started to lift the oil again. The residue had the characteristics of asphalt and was not recovered completely.

3.4 Burn 4

Starting with a base at 80 °C, addition of 200 mL water created a temperature gradient in the base from 40 °C at the surface to (estimated) 80 °C in the interior. The temperature gradient stabilized once 350 mL crude oil were added to the water surface. The burn lasted for 5:30 minutes, with the water starting to boil 5 minutes into the burn (i.e., vigorous burn phase or boil-over, Figure 2) at which time the surface temperature of the base had reached 70 °C. A rapid rise of the surface temperature was seen at the beginning of boil-over (20 °C in 20 seconds) and the highest temperature recorded in the base during boil-over was 90 °C. A thin film of residual oil remained on the water, and a small amount of oil was spread around the burn pan. Attempts to re-ignite the residual oil film were unsuccessful.

4 Discussion

Burn volumes and times show that the burn rates (oil regression rates) were between 1 and 2 mm/minute (Table 1), in-line yet at the high end of general expectations for oil fires of this pan size (Buist et al., 2013). Wind, which was present in gusts during the experiments, may have increased the burn rate (Buist et al., 2013).

The downward heat flux calculated from the block temperature at the center of oil pool is shown in Figure 4. While the development and magnitude of fluxes determined from Equations [3] and [4] agree with each other, the flux including the surface measurement, i.e. Equation [3], shows peaks and high-frequency variability that is absent in heat flux estimates based only on

temperature data from 5 mm and below (Equation [4]). The high-frequency variability may be exaggerated since the end of burn 2 due to surface damage the pan sustained. However, the close agreement between estimates in subsequent burn 3 (Figure 4c) suggests that this issue is minor.

The heat flux into the block increased as the respective burns continued, reaching 10 to 15 W/m^2 toward the end of burns 1 to 3. This is significantly below the black body radiation of 45 kW/m^2 at 680 °C (cf. Table 2). The surface temperature T_0 reached 300 °C during the Diesel burn which left no residue. Hence, the surface temperature of the Diesel pool was most likely also >300 °C, at least toward the end of the burn. This is a credible order of magnitude since the surface temperature of burning crude oil has previously been found to be between 200 and 300 °C (Buist et al., 2013). Quantitative interpretation of the burn process of burns 1 and 3 is handicapped by gas bubbles penetrating the oil layer during the later stages of the respective burns (cf. Results).

Prior to burn 4 the block was quite warm (70 °C), and a heat flux from the block to the water of 2 to 3 kW/m^2 was observed after water was added to the pan (Figure 4d). At the same time, the temperature at the pan surface (T_0) increased by 15 °C over the course of 160 seconds. Assuming this temperature represents the temperature of the well-mixed water layer above of 0.006 m thickness (Table 1), this rate of temperature increase would require a heat flux into the water of 2.4 kW/m^2, compatible with the heat flux estimate from the enthalpy development in the block. The temperature T_0 drops briefly and then remains stable at 40 °C following the addition of cold oil (10 °C) to the pan, i.e. the oil layer is cooling the water at the same rate the block is warming it. The oil pool was ignited shortly thereafter, and starting 4.5 minutes later the direction of heat transfer reversed with the water heating the block. As a result, the water layer may have been heated stably stratified until boiling started when the temperature T_0 rose rapidly from 70 °C to 90 °C (i.e., within 20 seconds, starting 6 minutes after ignition). The heat flux into the block just prior to vigorous burning was 1 kW/m^2. This is the same order of magnitude as the conductive heat flux estimate into a much larger oil pool burning on water of Evans et al. (1988), which was 2.5 kW/m^2. Since the upper water surface can reach temperatures around 100 °C at the most, the heat flux observed here may have been limited by the high temperature of the block (compared with, for example, surface seawater). In the present experiments, the heat flux reached 5 to 6 kW/m^2 during the vigorous burning phase. That heat input decreased only slowly after the end of the burn since the layer of hot water remained in contact with the block.

The efficiency of burn 1 was 83%. However, the burn efficiency may have been higher had re-ignition been attempted. If bubble formation was due to water vapor emanating from the base (rather than, for example, boiling of saturates), the flame could have extinguished in response to water vapor permeating the oil. The source of the water vapor would have been the recently cast mortar block as it heated up beyond 100 °C.

While mortar is a convenient material for construction it takes months to cure completely. Burns were performed after only one week of settlement which could have resulted in changes of thermal properties over the course of the four burns (including water content). Attempts have therefore been made to improve the fit of the model to temperature data by fitting individual burns separately, and by including a liquid–vapor phase transition in the thermal model. However, results obtained were not conclusive in that they neither pointed at crucial processes that are lacking in the simple thermal model (Equation 1), nor did they reveal a gradual, monotonic change of thermal properties of the mortar. Therefore, the model was run with constant thermal properties to estimate the heat content of the bottom of the mortar block.

5 Conclusion

The downward conductive heat flux into the ground was estimated for oil burns in a pan integrated in a mortar block instrumented with thermocouples.

Estimates of the net downward heat flux were obtained for an oil pool fire of 200 mm diameter. The heat flux into the base was 10 to 15 kW/m^2 for 200 mm oil pools on a solid surface. The heat flux was 1 kW/m^2 for an oil pool atop a 6-mm water layer prior to vigorous burn and increased to 5 to 6 kW/m^2 during vigorous burn. However, the latter numbers give only an approximate indication as the starting temperature of the base and water were very high compared with burns on open ocean or on ice.

6 Acknowledgements

The experiments were supported by the Nordland County Council, Norway. Troll B crude oil was kindly provided by Equinor (formerly Statoil).

7 References

Bellino, P., M. Flynn, and A.S. Rangwala. “A study of in-situ burning of crude oil in an ice channel”. Proceedings of the Combustion Institute 34(2):2539–2546, 2013.

Buist, I.A, S.G. Potter, B.K. Trudel, S.R. Shelnutt, A.H. Walker, D.K. Scholz, P.J. Brandvik, J. Fritt-Rasmussen, A.A. Allen, and P. Smith. “In Situ Burning in Ice-Affected Waters: State of knowledge report”. Final report 7.1.1. Report from Arctic Oil Spill Response Technology Joint Industry Programme (JIP). 294 pp., 2013.

Evans, D.D., G. Mulholland, D. Gross, H. Baum, and K. Saito. “Burning, Smoke Production, and Smoke Dispersion from Oil Spill Combustion”. In Proceedings of the Eleventh Arctic and Marine Oilspill Program (AMOP) Technical Seminar, June 7-9, Vancouver, BC. Environment Canada, Ottawa, ON, Canada, pp. 41-87, 1988.

Farahani, H.F., W.U.R. Alva, A.S. Rangwala, and G. Jomaas. “Convection-driven melting in an n-octane pool fire bounded by an ice wall”, Combustion and Flame, 179, 219-227. https://doi.org/10.1016/j.combustflame.2017.02.006, 2017.

Garo, J.P., J.P. Vantelon, S. Gandhi, and J. L. Torero. "Determination of the Thermal Efficiency of Pre-boilover Burning of a Slick of Oil on Water", Spill Science & Technology Bulletin, 5:2:141-151, 1999.

NORCOR. “The interaction of crude oil with Arctic sea ice”. Beaufort Sea Project NORCOR Engineering & Research Ltd, Technical report no. 27, Canada Department of the Environment, Victoria, British Colombia. 213 pp, 1975.

Shi, X., R.T. Ranellone, H. Sezer, N. Lamie, L. Zabilansky, K. Stone, and A.S. Rangwala. Influence of ullage to cavity size ratio on in-situ burning of oil spills in ice-infested water, Cold Regions Science and Technology, 140, 5-13. https://doi.org/10.1016/j.coldregions.2017.04.010, 2017.

8 Figures

Figure 1. Block with burn pan prior to burn.

Figure 2. Vigorous burn phase at the end of burn 4. Note the water droplets in front of the black shield to the left (white cloud).

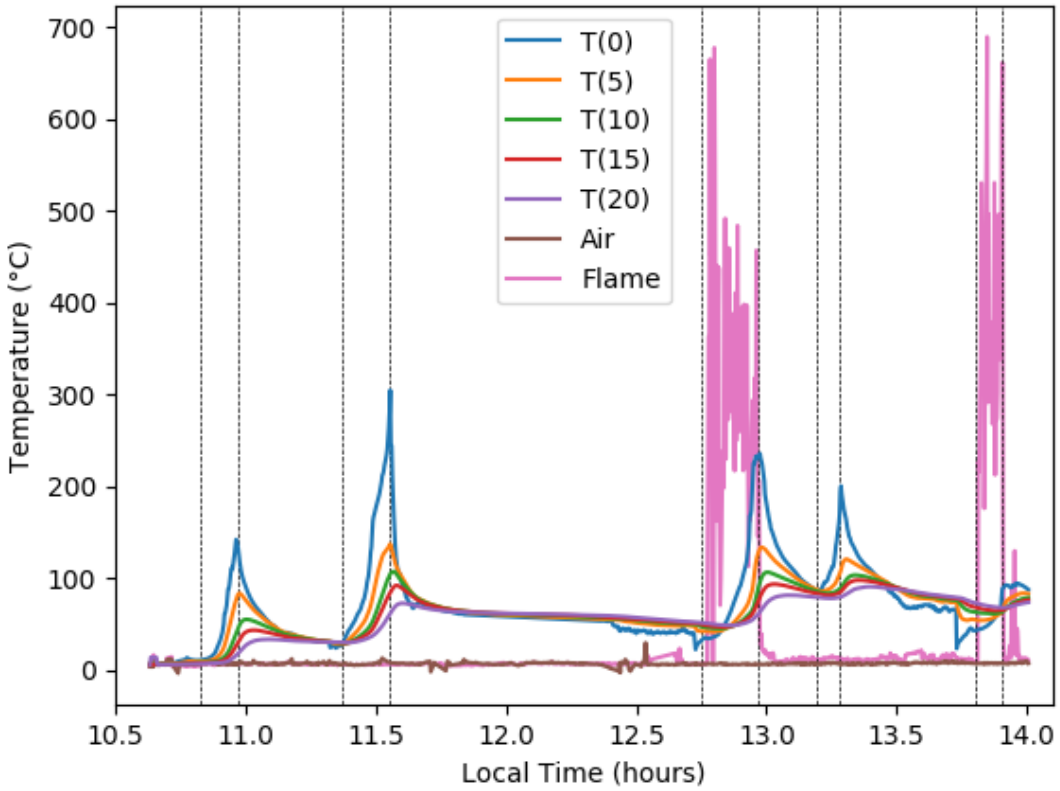

Figure 3. Overview of temperature measurements. The vertical dotted lines indicate start and end of burn 1, burn 2, burn 3, the re-ignition and associated burn of oil following burn 3, and burn 4. Flame temperature was measured during burns 3 and 4, only.

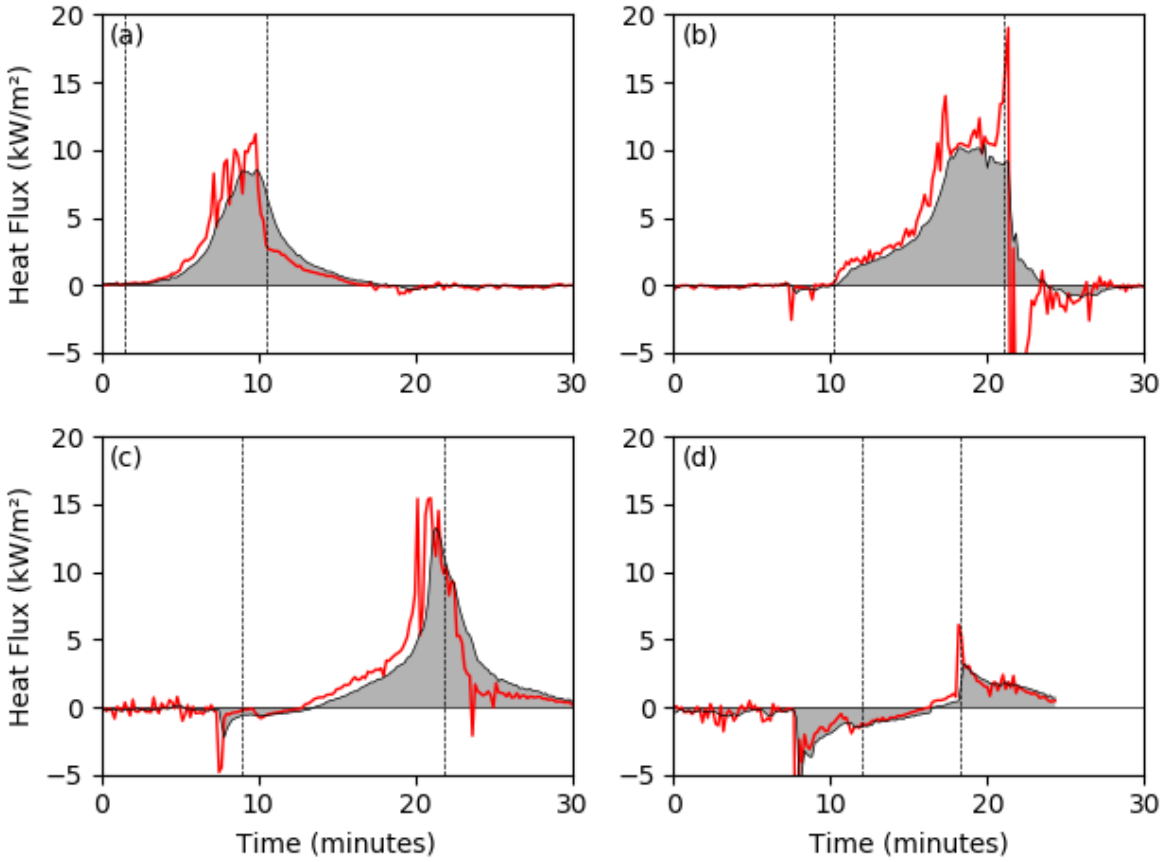

Figure 4. Net heat flux into the base of (a) burn 1, (b) burn 2, (c) burn 3, and (d) burn 4. The vertical lines indicate the periods of burn. The red line and gray patch show the heat flux based on Equations [3] and [4], respectively. Note that the most efficient heat transfer starts in the vigorous burn phase in burn 4.

9 Tables

Table 1. Overview parameters of the burns: amount of liquid, the corresponding film thickness in the pan, actual time of burn, description of the residue, and maximum flame height

	Liquid	Amount (mL)	Thickness (mm)	Burn time (min)	Residue	Max. flame height (m)
1	Crude Oil	500	16	9	liquid, more viscous than prior to burn	0.5
2	Diesel	450	14	12	none	0.5
3	IFO 60	500	16	13+1	asphalt	0.3
4	Crude Oil + Water	350 200	11 6	5.5	thin oil film on water	>1.2

Table 2. Measured temperatures of the base and derived heat flux below the pan. Flame temperature is the maximum value measured at a single-point

	Initial block temperature (°C)	Max. pan surface temperature (°C)	Measured flame temperature (°C)	Net heat flux (kW/m^2)
1	7	140	n/m	10
2	30	300	n/m	10
3	50	230	680	15
4	40-70	67*	680	1*

n/m: not measured

* prior to boil-over. Reaching 90 °C and 5 kW/m^2 during boil-over